Co-production of light p-, s- and r-process isotopes in the high-entropy wind of type II supernovae

K. Farouqi[A], *K.-L. Kratz*[B,C] *and B. Pfeiffer*[B]

[A] Department of Astrophysics and Astronomy, University of Chicago, Chicago, IL 60637, USA

[B] Max-Planck-Institut für Chemie, Otto-Hahn-Institut, D-55128 Mainz, Germany

[C] Email: kratz@mpch-mainz.mpg.de

Abstract:

We have performed large-scale nucleosynthesis calculations within the high-entropy-wind (HEW) scenario of type II supernovae. The primary aim was to constrain the conditions for the production of the classical "p-only" isotopes of the light trans-Fe elements. We find, however, that for electron fractions in the range $0.458 \leq Y_e \leq 0.478$, sizeable abundances of p-, s- and r-process nuclei between ^{64}Zn and ^{98}Ru are coproduced in the HEW at low entropies ($S \leq 100$) by a primary charged-particle process after an α-rich freezeout. With the above $Y_e - S$ correlation, most of the predicted isotopic abundance ratios within a given element (e.g. ^{64}Zn(p)/^{70}Zn(r) or ^{92}Mo(p)/^{94}Mo(p)), as well as of neighboring elements (e.g. ^{70}Ge(s+p)/^{74}Se(p) or ^{74}Se(p)/^{78}Kr(p)) agree with the observed Solar-System ratios. Taking the Mo isotopic chain as a particularly challenging example, we show that our HEW model can account for the production of all 7 stable isotopes, from "p-only" ^{92}Mo, via "s-only" ^{96}Mo up to "r-only" ^{100}Mo. Furthermore, our model is able to reproduce the isotopic composition of Mo in presolar SiC X-grains.

Keywords: nucleosynthesis – supernovae – high-entropy wind – isotopic abundances

1 Introduction

The origin of the stable isotopes of the light trans-Fe elements in the Solar System (SS) has been a fascinating area for nuclear astrophysicists over more than 50 years. It is commonly believed that these elements (between Zn (Z=30) and about Cd (Z=48)) are produced by varying contributions from three historical nucleosynthesis processes, (i) the "p-process" (see, *e.g.* Burbidge et al. (1957); Arnould (1976); Woosley & Howard (1978)), (ii) the "weak s-process" (see, *e.g.* Clayton (1968); Käppeler et al. (1982); Käppeler, Beer & Wisshak (1989)), and (iii) the "weak r-process" (see, *e.g.* Seeger, Fowler & Clayton (1965); Hillebrandt (1978); Cowan, Thielemann & Truran (1991); Kratz et al. (1993)).

Apart from the SS **isotopic** abundances (Lodders 2003), astronomical observations in recent years of **elemental** abundances in ultra-metal-poor (UMP) halo stars (see, *e.g.* Barklem et al. (2005); François et al. (2007); Mashonkina et al. (2007)) revived and intensified interest in the nucleosynthesis of these elements, and have motivated various theoretical studies with increasing realism (see, *e.g.* Hoffman et al. (1996); Rauscher et al. (2002); Travaglio et al. (2004); Fröhlich et al. (2006); Farouqi et al. (2008a,b); Kratz et al. (2008); Pignatari et al. (2008); Wanajo et al. (2009); Farouqi et al. (2009)). In addition, measurements of the **isotopic** compositions of trans-Fe elements in presolar SiC grains of type X (see, *e.g.* Pellin et al. (2000, 2006); Marhas, Hoppe & Ott (2007)), motivated a suggestion for a fourth process contributing to these isotopes, i.e. a neutron burst in the shocked He shell of a supernova (Meyer, Clayton & The 2000). However, even those recent models have ma-

jor shortcomings the one or other way. In particular, as in the older models, still none of the presently favored astrophysical scenarios produces sufficiently high abundances of all p-nuclei of Zn (Z=30) to Ru (Z=44), and all models seem to be unable to reproduce the SS abundance ratio of the two highly abundant p-isotopes ^{92}Mo and ^{94}Mo (Lodders 2003).

The high-entropy wind (HEW) of core-collapse type II supernovae (SN II) may offer a solution to the above problems by producing the light trans-Fe elements by a primary charged-particle (α-) process. This nucleosynthesis process seems to be largely uncorrelated (Zn – Mo) or weakly correlated (Mo – Cd) with the "main" r-process at and beyond the A$\simeq$130 abundance peak (Woosley & Hoffman 1992; Qian & Wasserburg 2007; Hoffman et al. 2008; Farouqi et al. 2008a,b; Kratz et al. 2008; Farouqi et al. 2009), as is indicated by recent astronomical observations. In the present paper, we describe under which conditions of electron abundance (Y_e=Z/A), entropy (S$\sim$Tρ [k$_b$/baryon]) and a selected expansion speed of the ejecta (V_{exp}=7500 [km/s]), the HEW scenario can co-produce p-, s- and r-process isotopes of the trans-Fe elements between Zn (Z=30) and Ru(Z=44). We present absolute yields in units of M$_\odot$ for a pure charged-particle (α-) process for the choice of three typical electron abundances of Y_e=0.450, 0.470 and 0.490.

Furthermore, we show for a number of selected cases that the predicted isotopic abundance ratios within a given element (e.g. ^{64}Zn(p)/^{70}Zn(r)), as well as of neighboring elements (e.g. ^{70}Ge(s+p)/^{74}Se(p)) agree well with the observed SS abundance ratios. However, as in other models, we cannot completely avoid cer-

tain isotopic over-abundances (e.g. for ^{88}Sr and ^{90}Zr) or under-abundances (e.g. for ^{96,98}Ru).

Taking the Mo isotopic chain as a particularly challenging example, we show that the α-component of our HEW model can account for the production of all seven stable isotopes, from "p-only" ^{92}Mo, via "s-only" ^{96}Mo up to "r-only" ^{100}Mo. Finally, we indicate that our model is also able to reproduce the isotopic composition of Mo in presolar SiC X-grains, recently measured by (Pellin et al. 2000, 2006).

Unlike the "neutron-burst" model of (Meyer, Clayton & The 2000) and the "γ-process" in the pre-SN and SN models of (Rauscher et al. 2002) (which both start from an initial SS "seed" composition); however similar to the "neutrino-wind" model of (Hoffman et al. 1996) and the recent "electron- capture SN" model of (Wanajo et al 2009), the α-component of our HEW scenario is a **primary** process. This means that the low-S production of all light trans-Fe isotopes (classical p-, s- and r) does not require any assumptions about the initial composition of the SN progenitor star.

2   Calculations and Results

The concept of a high-entropy wind (HEW) arises from considerations of the newly born proto-neutron star in core-collapse supernovae. In this scenario, the late neutrinos interact with matter of the outermost neutron-star layers, leading to moderately neutron-rich ejecta with high entropies (see, *e.g.* Woosley et al. (1994); Hoffman et al. (1996); Freiburghaus et al. (1999); and for recent publications, see, *e.g.* Heger & Woosley (2008); Hoffman, Müller & Janka (2008), and references therein). As in (Farouqi et al. 2008a,b, 2009), in the calculations presented here we follow the description of adiabatically expanding mass zones as previously utilized in (Freiburghaus et al. 1999). The nucleosynthesis calculations up to the charged-particle freezeout were performed with the latest Basel code, but without taking into account neutrino-nucleon / nucleus interactions. Neutrino-accelerated nucleosynthesis, the so-called (νp)-process (see, *e.g.* Fröhlich et al. (2006)) produces proton-rich matter and drives the nuclear flow into the "light" trans-Fe region, contributing considerably to the production of elements up to the Zn (Z=30) – Ge (Z=32) region, but then presumably fading out quickly in the Se (Z=34) – Rb (Z=37) region. (Fröhlich et al. 2006) predict that the νp-process would also efficiently synthesize p-nuclei between Sr (Z=38) and Pd (Z=46). However, we believe that with more realistic neutrino fluxes, the νp-process will not contribute significantly to the "heavier" trans-Fe elements. Therefore, we assume that these elements are primarily produced by the charged-particle (α-) component of the HEW.

Reaction rates for the HEW model were taken from the Hauser-Feshbach model NON-SMOKER (Rauscher & Thielemann 2000; Rauscher 2007). The subsequent parameterized "r-process" network calculations use updated experimental and theoretical nuclear-physics input on masses and β-decay properties, as outlined in (Kratz 2007a) and used in our earlier "waiting-point" calculations

(see, *e.g.* Kratz et al. (1993); Kratz, Farouqi & Pfeiffer (2007b)).

After charged-particle (α-) freezeout, the expanding and eventually ejected mass zones have different initial entropies (S), so that the overall explosion represents a superposition of entropies correlated with different electron abundances (Y_e), different ratios of free neutrons to "seed" nuclei (Y_n/Y_{seed}), and eventually different expansion velocities (V_{exp}) as well (Farouqi et al. 2008a,b; Kratz et al. 2008). If one assumes that equal amounts of ejected material per S-interval are contributing, the sum of these abundance fractions is weighted according to the resulting Y_{seed} as a function of S (see, *e.g.* Fig. 1 in Farouqi et al. (2008a) and / or Farouqi et al. (2009)). From this parameter study, we have found that the HEW predicts – at least – two clearly different nucleosynthesis modes. For low entropies (e.g. $5 \leq S \leq 110$ at Y_e=0.450), the concentration of free neutrons is negligible. Hence, the nucleosynthesis in this S-range is definitely not a neutron-capture process but rather a charged-particle (α-) process. For higher entropies, the Y_n/Y_{seed} ratios are increasing smoothly, resulting in a neutron-capture component resembling a classical "weak" r-process followed by the classical "main" r-process, which produces the heavy nuclei up to the Th, U actinide region.

In our previous papers (Farouqi et al. 2008a,b; Kratz et al. 2008; Farouqi et al. 2009), we have compared our HEW model results to the classical SS **isotopic** "r-residuals" ($N_{r,\odot} = N_\odot - N_s$; (see, e.g. Käppeler, Beer & Wisshak (1989); Arlandini et al. (1999)) and to recent **elemental** abundances in UMP halo stars (see, e.g. Barklem et al. (2005); Cowan & Sneden (2006); Mashonkina et al. (2007)). In these papers we have demonstrated that a superposition of entropies in the full range of $5 \leq S \leq 300$ for a single electron fraction of Y_e=0.450 was able to very well reproduce the SS "main" r-process distribution in the mass range $120 \leq A \leq 209$ (see, e.g. Fig. 2 in Kratz et al. (2008) and / or Farouqi et al. (2009)). However, it also became obvious that this way of weighting the S-components for a single Y_e value did not fit the classical "r-residuals" in the region between the Fe-group and the rising wing of the A$\simeq$130 peak, neither for the SS isotopic abundances, nor for the element abundances in the majority of the UMP stars. In particular for the light trans-Fe elements of Zn (Z=30) to Rb (Z=37) in these stars, it was evident that the HEW model predicts much too low Z-abundances (see, e.g. Fig. 3 in Kratz et al. (2008) and / or Farouqi et al. (2009)).

There have been several suggestions to explain the abundances in this mass region with a multiplicity of nucleosynthesis processes. The first authors who recognized this possibility were (Hoffman et al. 1996) with their neutrino-driven wind model (see also Hoffman, Woosley & Qian (1997)). In this parameter study, with the restriction to a single low entropy of S$\simeq$50 and a variety of electron fractions in the range $0.46 \leq Y_e \leq 0.50$, they noted that *"the r-process and some light p-process nuclei may be coproduced"* in a primary charged-particle process. Later, after the first measurements of some elements in the trans-Fe region of UMP halo stars had become

available, a light element primary process "LEPP" was invoked by (Travaglio et al. 2004), qualitatively related to s-like neutron captures. A recent more quantitative alternative to such a neutron-capture scenario could be a strong secondary s-process with a primary (α,n) neutron source in massive stars at low metallicities, as suggested by (Pignatari et al. 2008). On the other hand, in the latest revised version of the phenomenological "LEGO" model of (Qian & Wasserburg 2007; Waserburg & Qian 2009), following the basic arguments of (Hoffman et al. 1996), consider the trans-Fe elements to be dominantly produced by charged-particle reactions.

As already discussed in previous papers (see, e.g.Farouqi et al. (2008a,b); Kratz et al. (2008); Farouqi et al. (2009)) our HEW approach with the above parameter choices of individual Y_e and V_{exp} and superpositions of S did neither fully support the above "LEPP" nor the "LEGO" idea. We have shown that the low-S region (S≤100 for a Y_e=0.45), is indeed a pure charged-particle process, producing the lighter trans-Fe elements up to about Nb (Z=41). This is in agreement with the initial ideas of (Hoffman et al. 1996) and the later "LEGO" approach, but in disagreement with the "LEPP" idea. From Mo (Z=42) on upwards, however, our HEW model predicts smoothly increasing fractions of neutron-capture material, now in qualitative agreement with the "LEPP" approach, but in disagreement with the "LEGO" picture.

After having focussed on *elemental* abundances in the past, in this paper we want to discuss first HEW results on *isotopic* abundances of the trans-Fe elements between Zn (Z=30) and Ru (Z=44), in particular their decomposition into the respective fractions of the historical p-, s- and r-process nuclei. We start by presenting in Table 1 the isotopic abundances between ^{64}Zn and ^{98}Ru in units of solar masses $M_\odot$ for three typical neutrino-wind conditions. For a selected expansion velocity of V_{exp}=7500 [km/s], we consider for the other two correlated parameters (i) a "neutron-rich" component with Y_e=0.450 and an entropy superposition of 5≤ S ≤100 (S≤100), (ii) a "proton-rich" component with Y_e=0.490 and a superposition of S≤150, and (iii) a "medium" component with Y_e=0.470 and a superposition of S≤120, where the maximum entropy for each value of Y_e is defined by a neutron-to-seed ratio Y_n/Y_{seed}=1.0. With these parameter choices only the charged-particle (α-) component of the total HEW abundances is considered.

Several conclusions can be drawn from our detailed HEW model calculations in the total $Y_e - S - V_{exp}$ parameter range. The first one is, that the overall yields of the light trans-Fe elements decrease with increasing Y_e. When considering the total Z-region between Fe and Cd, the produced α-yields are about $4.0\text{x}10^{-3}$ $M_\odot$ for Y_e=0.450 and $2.7\text{x}10^{-3}$ $M_\odot$ for Y_e=0.490, respectively. These abundances can be compared with the corresponding neutron-capture r-process yields (for higher entropies with corresponding Y_n/Y_{seed} >1.0) of $3.4\text{x}10^{-4}$ $M_\odot$ for Y_e=0.450 and $4.3\text{x}10^{-5}$ $M_\odot$ for Y_e=0.490, respectively. The second observation is, that in the range 0.450≤Y_e≤0.480 the relative isotopic abundances of the trans-Fe elements are shifted towards the lighter

stable nuclides favoring s-iotopes, or even to the proton-rich side then favoring p-isotopes. For higher electron abundances up to Y_e=0.498, the trend becomes slightly reverse.

Furthermore, for the range 0.460≤Y_e≤0.490 the HEW low-entropy charged- particle (α-) process produces the lightest isotopes of all even-Z isotopes between Fe (Z=26) and Ru (Z=44), where all p-nuclei are involved. Above Ru (Z=44), the abundance fractions of the HEW α-component become negligible compared to the now dominating neutron-capture "weak" r-process. Hence, sizeable isotopic yields for Pd (Z=46) and Cd (Z=48) are only produced for the heavier isotopes ^{105}Pd and ^{111}Cd and beyond, respectively.

For a more quantitative consideration, let us choose as typical examples the HEW α-process yield ratios of the two lightest isotopes of Zn, (i.e. ^{64}Zn/^{66}Zn), Sr, (i.e. ^{84}Sr/^{86}Sr), and Mo, (i.e. ^{92}Mo/^{94}Mo) (see Table 1). As can be deduced from Table 1, the predicted yield ratio of ^{64}Zn/^{66}Zn varies between $9.5\text{x}10^{-3}$ for Y_e=0.450, 1.02 for Y_e=0.470 and 1.57 for Y_e=0.490, where the isotopic ratio for "moderate" Y_e values slightly above 0.47 seem to agree best with the measured SS yield ratio of 1.74 of (Lodders 2003). The dominant effect in the HEW ratios comes from the strong increase of the ^{64}Zn yield by roughly two orders of magnitude in the 0.45≤Y_e≤0.47 range, whereas the corresponding change of the ^{66}Zn abundance is only a factor 2. A similar picture is obtained for the abundance ratio of ^{84}Sr/^{86}Sr, resulting in $2.0\text{x}10^{-4}$ for Y_e=0.450, $8.9\text{x}10^{-2}$ for Y_e=0.470 and $5.7\text{x}10^{-2}$ for Y_e=0.490. Here, the best agreement with the SS abundance ratio of $5.66\text{x}10^{-2}$ seems to be reached for a rather proton-rich Y_e scenario. Finally, the predicted abundance ratio of the two "p-only" isotopes ^{92}Mo and ^{94}Mo vary between 0.62 for Y_e=0.450, 13 for Y_e=0.470 and 9.6 for Y_e=0.490. In this case, none of the above HEW ratios agrees with the SS abundance ratio of 1.60.

From the above results deduced from Table 1, we see that with this rather coarse HEW parameterization we do not obtain a consistent picture for the whole trans-Fe region. This seems to confirm all earlier and recent attempts which also were not able to obtain a satisfactory overall reproduction of the SS abundances in the region of the light trans-Fe p-nuclei the one or other way (see, e.g. Hoffman et al. (1996); Hoffman, Woosley & Qian (1997); Meyer, Clayton & The (2000); Rauscher et al. (2002); Hoffman, Müller & Janka (2008); Bazin et al. (2008); Pignatari et al. (2008); Fisker, Hoffman & Pruet (2009); Wanajo et al. (2009)). Therefore, two further refinements of our model may be necessary to improve the situation obtained so far: (i) a finer grid of *individual* values of Y_e in the range 0.450≤Y_e≤0.490, and / or (ii) a *superposition* of Y_e values with model-inherent weighting of the respective HEW yields.

We have followed both approaches successively. And, already with a finer grid of single Y_e trajectories and the previously applied S-superposition up to S_{max} where Y_n/Y_{seed}=1.0, in a large number of cases we obtain isotopic abundance ratios for a specific element and for nuclides of neighboring elements which are in bet-

ter agreement with the SS values. However, as shown for example by (Burrows et al. 2007), even more realistic should be an additional weighted superposition of Y_e trajectories over certain ranges. In the following, in Table 2 we present our first HEW results from the second approach with correlated superpositions of S and Y_e on selected isotopic abundance ratios. In our attempt to obtain a consistent overall reproduction of the SS values, we have determined the optimum ranges of the two astrophysical parameters for the later model-inherently weighted superposition. As already mentioned before, we have restricted our study to the full entropy ranges (S≤100 for Y_e=0.45, S≤120 for Y_e=0.47 and S≤150 for Y_e=0.49) responsible for a pure charged-particle (α-) process. Within these S-ranges, a rather constant range of 0.458≤Y_e≤0.474 has been obtained for the whole mass region from Zn up to Ru. With this optimized, correlated S – Y_e superposition, we have compared our predictions with the three selected nucleosynthesis models of (Hoffman et al. 1996), (Rauscher et al. 2002) and (Wanajo et al. 2009).

It is evident from our Table 2, that – as attempted by our above parameter "finetuning" – in most of the cases, the isotopic abundance ratios of our HEW α-component agree quite well with the SS values. Exceptions are indicated by (i) the "step" of about a factor 4 for the two p-nuclei ^{74}Se/^{78}Kr, (ii) the well known local over-abundances in the N=50 region for Sr and Zr isotopes, and (iii) the low abundances of the two p-isotopes of Ru, their abundance ratio, however, again agreing with the SS ratio. Nevertheless, compared to the other three models, our low-S HEW α-process gives the best overall agreement with the SS isotopic abundance ratios.

In the early (Hoffman et al. 1996) parameter study on the *"production of the light p-nuclei in neutrino-driven winds"*, who use a single entropy of S≃50 and individual electron fractions in the range 0.46≤Y_e≤0.50, the authors have noted for the first time that their *"new kind of p-process"* is primary and that *"the r-process and some light p-process nuclei may be coproduced"*. With respect to Mo and Ru, (Hoffman et al. 1996) conclude that ^{92}Mo is made in quasi-equilibrium with ^{90}Zr, whereas *"the origins of ^{94}Mo and ^{96,98}Ru remain a mystery"*. For our comparison, we have deduced the available abundance ratios from their Fig. 3 (for Y_e=0.460) and their Table 4. It is evident from our Table 2 that, maybe except ^{70}Ge/^{74}Se and ^{92}Mo/^{94}Mo, there is no agreement between the ν-wind model and the SS values for all other abundance ratios of the light p-isotopes between Zn and Ru.

(Rauscher et al. 2002) have presented detailed nucleosynthesis calculations in massive stars from the onset of central H-burning through explosion of SN-II for Population I stars of 15≤$M_\odot$≤25. They find that in some stars, most of the p-nuclei can be produced in the convective O-burning shell prior to collapse, whereas others are made only in the explosion. Again, with respect to Mo and Ru, the authors point out that *"serious deficiencies still exist in all cases for the p-isotopes of Mo and Ru"*. For our comparison, we have chosen their 15 $M_\odot$ model S15 which starts with an initial SS "seed" composition, which is further modulated by an

s-process and finally by a γ-process. As can be seen from our Table 2, for the majority of the selected isotopic abundances, the above model gives quite good agreement with the SS values. Similar to our HEW model, a large abundance "step" is observed between Se and Kr, as well as the strong over-abundances in the N=50 Sr – Zr region. In addition, and in contrast to our HEW approach, the SS isotopic ratios in the Zn – Ge region cannot be reproduced.

A very recent state-of-the-art hydrodynamical simulation on the *"nucleosynthesis in electron-capture (EC) supernovae of asymptotic giant branch stars with an O–Ne–Mg core"* has been performed by (Wanajo et al. 2009). For electron fractions in the range 0.464≤Y_e≤0.470 the authors obtain large productions of light p-nuclei between ^{64}Zn and ^{92}Mo. The correlated significant overproduction of ^{90}Zr can be avoided in their model by *"boosting Y_e to 0.480"*. Another interesting result is that in their EC SN scenario obviously *"the νp-process does not play any role in producing the p-nuclei"*. For comparison with our results and the SS values, we have chosen the abundances from their unmodified model ST. As can be seen from our Table 2, agreement with the SS isotopic abundances is only obtained in a few cases. The most evident discrepancies obviously occur for the all neutron-rich (r-process) nuclides of Zn up to Zr, which are orders of magnitude under-produced relative to their p-isotopes. Also the SS value of ^{92}Mo/^{94}Mo cannot be reproduced.

Finally, we want to discuss explicitly the abundances of the Z=42 Mo isotopes predicted by the α-component of our HEW model. There are several reasons for chosing this isotopic chain. In the light trans-Fe region, besides Ru (Z=44), Mo has with 7 nuclides the longest sequence of stable isotopes, from the two light "p-only" nuclei ^{92}Mo and ^{94}Mo (with their unusually high SS fractions of 14.84% and 9.25%, respectively), via the intermediate-mass "s-only" isotope ^{96}Mo (16.68%), up to the "r-only" nuclide ^{100}Mo (9.63%) (Lodders 2003); the remaining isotopes ^{95,97,98}Mo have mixed s + r origin. Therefore, it is of special interest to check whether our HEW model can in principle account for the coproduction of all 7 stable Mo isotopes, and which abundance fractions relative to the SS values can be formed by the low-S charged-particle process. Another challenge is the recent observation of the peculiar Mo isotopic composition of some rare presolar SiC X-grains by (Pellin et al. 2000, 2006), which clearly differ from all classical nucleosynthesis processes.

Let us have a closer look, how the 7 stable Mo (Z=42) isotopes can be synthesized. Because of the specific position of Z=42 Mo in the chart of nuclides (see, *e.g.* Magill, Pfennig & Galy (2006)), in principle there exists only a narrow nucleosynthesis path for the Mo isotopes in between the stable Zr (Z=40) Zr and Ru (Z=44) isotopes. ^{92,94}Mo are shielded on the neutron-rich side by their isobars ^{92,94}Zr. Hence, the p-nuclide ^{92}Mo can only be produced directly or via β^+-decay from proton-rich isobars like ^{92}Tc. Apart from its direct synthesis as Mo isotope, the heavier p-nuclide ^{94}Mo can only be produced by β^+-decay of its proton-

rich isobars like ^{94}Tc and / or by β^--decay from ^{94}Nb. Only ^{95}Mo and ^{97}Mo can be reached by longer β-decay chains on both sides of stability. In contrast, the classicial s-only isotope ^{96}Mo in between is "shielded" on both sides by its stable isobars ^{96}Zr and ^{96}Ru. Finally, the two heaviest Mo isotopes, ^{98}Mo and the classical "r-only" nuclide ^{100}Mo, are again "shielded" on the proton-rich side by their Ru isobars, but can be reached by the full A=98 and 100 β^--decay chains on the neutron-rich side.

With this special situation for the different and possibly competing modes of populations, we now can check how the individual Mo isotopes are produced by the α-component of the HEW scenario. We find that the lightest stable Mo isotope is only formed directly as ^{92}Mo in the normal α-rich freezeout at low entropies of S$\leq$40. For ^{94}Mo (S$\leq$50) and ^{96}Mo (S$\leq$60), besides a predominant direct production, additional minor contributions in the A=94 mass chain come from β^+-decays of ^{94}Tc and ^{94}Ru, and in the A=96 chain from β^--decay of ^{96}Nb, respectively. No contributions are predicted by our HEW model from β^--decay of ^{94}Nb and from β^+-decay of ^{96}Tc. All other heavier Mo isotopes are no longer produced directly in significant amounts. They are instead predominantly formed as β^--decay end-products after an increasingly neutron-rich α-freezeout at somewhat higher entropies in the range 90$\leq$S$\leq$150 depending on Y_e. The main progenitors of ^{95}Mo are the β^--unstable isotopes ^{95}Y, ^{95}Zr and ^{95}Sr, with minor contributions from the even more neutron-rich isobars ^{95}Rb and ^{95}Kr. The latter two nuclides are already precursors of β-delayed neutron (βdn) emission (Pfeiffer, Kratz & Möller 2002). Their βdn-fractions will further β-decay to stable ^{94}Zr. For ^{97}Mo, the main isobaric progenitors are ^{97}Y, ^{97}Zr, ^{97}Sr and the βdn-precursor ^{97}Rb. The βdn-decay of this latter isotope will finally populate ^{96}Zr. In the A=97 mass chain, in addition small contributions to ^{97}Mo come from the βdn-decays of ^{98}Rb and ^{98}Kr. The nuclide ^{98}Mo is predominantly formed by the progenitor ^{98}Sr and to a minor extent by the two βdn-precursors ^{98}Rb and ^{98}Kr. Further small contributions come from the βdn-decays of ^{99}Rb and ^{99}Kr. Finally, the production of the "r-only" isotope ^{100}Mo within the A=100 mass chain originates exclusively from the neutron-rich progenitor ^{100}Sr; only small contributions come from very neutron-rich βdn-precursors of A=101.

The isotopic Mo abundances (Y(^{x}Mo)) predicted by the charged-particle (α-) component of our HEW model as a function of the electron abundance in the range 0.450$\leq$Y$_e$$\leq$0.498 (at V$_{exp}$=7500 km/s) are shown in Figure 1. For the whole Y$_e$-range, ^{96}Mo has the lowest yield of all Mo nuclei, followed by ^{94}Mo and ^{92}Mo. The abundances of ^{95,97,98,100}Mo are considerably higher and lie rather close together. They exhibit a smoothly decreasing pattern with increasing electron abundance up to Y$_e$$\simeq$0.490; for higher Y$_e$ the drop of their abundances becomes more pronounced and reaches – except for ^{95}Mo – the low values of ^{92,94}Mo. This drop in Y(^{x}Mo) in the range 0.490$\leq$Y$_e$$\leq$0.498 seems to be a general signature for all Mo isotopes. Whereas the abundance patterns of ^{94}Mo and ^{96}Mo are rather flat between Y$_e$=0.450 and about 0.490, ^{92}Mo
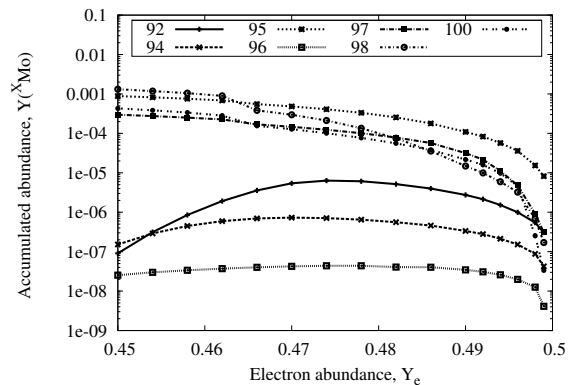

Figure 1: Isotopic Mo abundances Y(^{x}Mo) produced by the HEW α-process at an expansion velocity of V$_{exp}$=7500 km/s as a function of electron abundance in the range 0.450$\leq$Y$_e$$\leq$0.498. The symbols for the Mo isotopes are given in the upper part of the figure. For a discussion of the predicted abundance trends with Y$_e$, see text.

is the only nuclide which shows a more curved slope with its highest abundance around Y$_e$$\simeq$0.475.

In Figur 2, we show the isotopic abundance *ratios* of ^{x}Mo/^{97}Mo as a function of Y$_e$. Here we see that the ratios for the heavier s+r isotopes ^{95,97}Mo are quite flat over the whole Y$_e$-range. The "r-only" nuclide ^{100}Mo shows a similar behavior up to about Y$_e$$\simeq$0.490; then, the ^{100}Mo/^{97}Mo ratio increases towards Y$_e$=0.498. In contrast, the ^{x}Mo/^{97}Mo ratios of the two "p-only" isotopes ^{92,94}Mo and the "s-only" nuclide ^{96}Mo are smoothly increasing over the whole Y$_e$ range, with a steeper rise in their slopes at about Y$_e$$\geq$0.490.

As already mentioned in the introduction, still today the origin of the two p-nuclei ^{92}Mo and ^{94}Mo is considered to be *"one of the great outstanding mysteries in nuclear astrophysics"* (Fisker, Hoffman & Pruet 2009). Based on the initial ideas developed already 30 to 50 yeras ago (see, e.g. Burbidge et al. (1957); Arnould (1976); Woosley & Howard (1978)), more recently several astrophysical scenarios have been investigated in this special context, including for example a p-process based on photodisintegration of heavy elements produced by s- and r-processes (Arnould & Goriely 2003), core-collapse SNe with neutrino-wind, γ-process and νp- scenarios (see, e.g. Hoffman et al. (1996); Rauscher et al. (2002); Fröhlich et al. (2006); Fisker, Hoffman & Prue (2009)), EC SNe (Wanajo et al. 2009), and X-ray bursts (see, e.g. (Schatz et al. 1989; Weinberg, Bildsten & Schatz 2006)). However, none of these models has been able to reproduce consistently the high yields and the SS isotopic ratio of these two p-isotopes. Finally, also the neutron-capture "burst" model of (Meyer, Clayton & The 2000), which has originally been developed to explain the Mo isotopic composition in presolar SiC grains, fails to reproduce the SS ratio of $^{92}/^{94}$Mo.
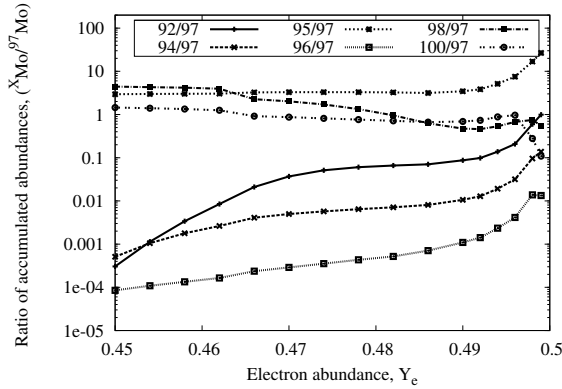
Figure 2: Isotopic abundance ratios of ^{x}Mo/^{97}Mo obtained for the HEW α-process at an expansion velocity of V_{exp}=7500 km/s as a function of electron abundance in the range $0.450 \leq Y_e \leq 0.498$. The symbols for the different isotopic ratios are given in the uppert part of the figure. For a discussion of the predicted trends with Y_e, see text.

To summarize this part, we conclude that the low-S charged-particle component of our HEW model co-produces all 7 Mo isotopes. With the above $S - Y_e$ superpositions, the SS isotopic ratio of ^{92}Mo/^{94}Mo is reproduced, whereas all other abundance ratios are different from the standard s-process and r-process values. While the yields of the isotopes ^{92,94,96}Mo have reached saturation already well below S_{max} (with Y_n/Y_{seed}=1.0), the production of the heavier, more neutron-rich nuclides ^{97,98,100}Mo continues to higher entropies, reaching the "weak" r-process component.

Last but not least, we want to present preliminary results of our HEW model which offers a new explanation of the puzzling Mo isotopic pattern in presolar SiC X-grains recently discovered by (Pellin et al. 2000, 2006). This pattern clearly differs from that derived from either a pure s-process or a classical r-process. So far, possible nucleosynthesis implications have only been successfully analyzed by (Meyer, Clayton & The 2000) within their neutron-capture scenario in shocked He-rich matter in an exploding massive star, among cosmochemists commonly cited as "neutron-burst" model. This rather complex model starts with a SS "seed" composition (thus initially containing already the "correct" SS abundances of the p-nuclei ^{92}Mo and ^{94}Mo), which is then exposed to a weak neutron fluence in order to mimic weak s-process conditions during the pre-SN phase. The weak-s ashes act as secondary seed composition, which are then suddenly heated to T_9=1.0. During expansion and cooling on a 10 s hydrodynamic timescale, a neutron density from (α,n) reactions of about 10^{17} n/cm^3 is created for about 1 s. Neutron density and burst duration are "finetuned" to transform the secondary seed composition in the Y to Mo region, so that simultaneously a large mass fraction

of ^{96}Zr is obtained, whereas all isotopes between ^{92}Mo and ^{97}Mo are strongly and ^{98,100}Mo are slightly depleted. With this kind of modulation of the seed abundances, the "neutron-burst" model yields good overall agreement with the Mo isotopic pattern of the SiC X-grains.

As already mentioned above, with our HEW model we have found that the isotopic abundances of the two "p-only" nuclides ^{92,94}Mo and the "s-only" isotope ^{96}Mo are already "saturated" well below S_{max} in the charged-particle (α-) component. Under these low entropy conditions ($5 \leq S \leq 70$), and within the correlated electron fractions in the range $0.456 \leq Y_e \leq 0.460$, we indeed obtain a consistent picture reproducing the SiC X-grain pattern.

Cosmochemists conventionally compare their measured isotopic abundance ratios with model predictions in terms of three-isotope mixing correlations, in order to describe the nucleosynthetic origin of their circumstellar grain material. Thereby, a best match of the model results to the grain data is deduced from mixing lines between the SS composition and the pure nucleosynthesis value (see, as an example the three-isotope plot of ^{100}Mo/^{97}Mo versus ^{96}Mo/^{97}Mo in Fig. 1 of Marhas, Hoppe & Ott (2007)). In Table 3 we compare the end members of the mixing lines of the SiC grain data with the predictions of the "neutron-burst" model and our HEW α-nucleosynthesis component with the above $S - Y_e$ superpositions. It is evident from this table, that our HEW approach of synthesizing all 7 Mo isotopes in the presolar SiC grains by a primary charged-particle process is (at least) an alternative to the secondary production by the "neutron-burst" model. However, an advantage of our approach may in principle be the agreement with the astronomical observations of the charged-particle nucleosynthesis mode of the light trans-Fe elements in UMP halo stars.

3   Summary and conclusion

We have shown in a large-scale parameter study that the high-entropy wind (HEW) scenario of type II supernovae can co-produce the light p-, s- and r-process isotopes between Zn (Z=30) and Ru (Z=44) at electron abundances in the range $0.450 \leq Y_e \leq 0.498$ and low entropies of $S \leq 100$–150. Under these conditions, the light trans-Fe elements are produced in a charged-particle (α-)process, including all p-nuclei up to ^{96,98}Ru. In our model, no initial SS, s- or r-process seed composition is invoked; hence, this nucleosynthesis component is primary. These results provide a means to substantially revise the abundance estimates of different primary and secondary nucleosynthesis processes in the historical "weak-s" and "weak-r" process regions. Chosing the Mo isotopic chain as a particularly interesting example, we have found that our HEW model can account for the simultaneous production of all 7 stable Mo nuclides, from p-only ^{92}Mo, via s-only ^{96}Mo up to r-only ^{100}Mo. Furthermore, we have shown that our model is able to reproduce the SS abundance ra-

tio of the two p-nuclei ^{92}Mo and ^{94}Mo. Finally, the likely nucleosynthesis origin of the peculiar Mo isotopic composition of the presolar SiC X-grains measured by (Pellin et al. 2000, 2006) has been determined.

To obtain more quantitative answers to questions concerning the astrophysical site(s) of the light trans-Fe elements will require on the one hand more and higher-quality observational data and on the other hand more realistic hydrodynamical nucleosynthesis calculations. In particular, it has to be studied in detail how severe overproductions of the SS abundances between Sr (Z=38) and Cd (Z=48) can be avoided when combining the partly high yields of all presently favored contributing processes for the trans-Fe elements, i.e. the early νp-process (Fröhlich et al. 2006), the subsequent HEW charged-particle process after normal and neutron-rich α-freezeout, possible ejecta from X-ray bursts (Weinberg, Bildsten & Schatz 2006) and the new strong s-process predicted to occur in massive stars at halo metallicity (Pignatari et al. 2008).

Acknowledgments

References

Arlandini, C. et al. 1999, Ap. J., 525, 886

Arnould, M. 1976, A&A, 46, 117

Arnould, M. & Goriely, S. 2003, Phys. Rep. 384, 1

Barklem, P.S. et al. 2005, A&A, 439, 129

Bazin, D. et al. 2008, Phys. Rev. Let., 101, 252501

Burbidge, E.M. et al. 1957, Rev. Mod. Phys., 29, 547

Burrows, A. et al. 2007, Ap. J., 655, 416

Clayton, D.D. 1968, Principles of Stellar Evolution and Nucleosynthesis, McGraw Hill, New York

Cowan, J.J., Thielemann, F.-K. & Truran, J.W. 1991, Phys. Rep., 208 (4&5), 267

Cowan, J.J. & Sneden, C. 2006, Nature, 440, 1151

Farouqi, K. et al. 2008, AIP Conf. Proc., 990, 309

Farouqi, K. et al. 2008, AIP Conf. Proc., 1001, 245

Farouqi, K. et al. 2009, Ap. J., 694, L49

Fisker, J.L., Hoffman, R.D. & Pruet, J. 2009, Ap. J., 690, L135

François, P. et al. 2007, A&A, 476, 935

Freiburghaus, C. et al. 1999, Ap. J. 516, 381

Fröhlich, C. et al. 2006, Ap. J., 644, 1028

Heger, A. & Woosley, S.E. 2008, arXiv:0803.3161

Hillebrandt, W. 1978, Space Sci. Rev., 21, 639

Hoffman, R.D. et al. 1996, Ap. J., 460, 478

Hoffman, R.D., Woosley, S.E. & Qian, Y.-Z. 1997, Ap. J., 482, 951

Hoffman, R.D., Müller, B. & Janka, H.-T. 2008, Ap. J., 676, L127

Hoffman, R.D. et al. 2008, AIP Conf. Proc., 1005, 225

Käppeler, F. et al., 1982, Ap. J., 252, 827

Käppeler, F., Beer, H. & Wisshak, K. 1989, Rep. Prog. Phys., 52, 945

Kratz, K.-L. et al. 1993, Ap. J., 403, 216

Kratz, K.-L. 2007, Ap. J., 662, 39

Kratz, K.-L., Farouqi, K. & Pfeiffer, B. 2007, Prog. Particle and Nucl. Physics, 59, 147

Kratz, K.-L. et al. 2008, New Astronomy Reviews 52, 390

Lodders, K. 2003, Ap. J., 591, 1220

Magill, J. Pfennig, G. & Galy, J. 1998, Chart of the Nuclides, 7th Edition 2006

Marhas, K.K., Hoppe, P. & Ott, U. 2007, Meteoritics & Planet. Sci., 42 (7&8), 1077

Mashonkina, L.I. et al. 2007, Astron. Rep., 51, 903

Meyer, B.S., Clayton, D.D. & The, L.-S. 2000, Ap. J., 540, L52

Pellin, M.J. et al. 2000, Lunar Planet. Sci. Conf., 31, 1917

Pellin, M.J. et al. 2006, Lunar Planet. Sci. Conf., 37, 2041

Pfeiffer, B., Kratz, K.-L. & Möller, P. 2002, Prog. Nucl. Energy 41, 39.

Pignatari, M. et al. 2008, Ap. J., 687, L95

Qian, Y.-Z. & Wasserburg, G.J. 2007, Physics Reports, 442, 237

Rauscher, T. & Thielmann, F.-K. 2000, ADNDT 75, 1 (2000)

Rauscher, T. et al. 2002, Ap. J., 576, 323

Rauscher, T. 2007, http://download.nucastro.org/astro/reaclib/

Schatz, H. et al. 1989, Phys. Rep. 294, 167

Seeger, P.A., Fowler, W.A. & Clayton, D.D. 1965, Ap. J. Suppl., 11, 121

Travaglio, C. et al. 2004, Ap. J., 601, 864

Wanajo, S. et al. 2009, Ap. J., 695, 208

Wasserburg, G.J. & Qian, Y.-Z. 2009, PASA, this volume

Weinberg, N.N., Bildsten, L. & Schatz, H. 2006, Ap. J. 639, 1018

Woosley, S.E. & Hoffmann, R.D. 1992, Ap. J. 395, 202

Woosley, S.E. & Howard, W.M. 1978, Ap. J. Suppl., 36, 285

Woosley, S.E. et al. 1994, Ap. J., 433, 229

Table 1: Yields of stable isotopes (in units of $M_\odot$) for the α-component of the HEW

Y_e=0.450		Y_e=0.470		Y_e=0.490	
Isotope	Yield $[M_\odot]$	Isotope	Yield $[M_\odot]$	Isotope	Yield $[M_\odot]$
^{64}Zn	.34E-06	^{64}Zn	.56E-04	^{64}Zn	.96E-05
^{66}Zn	.35E-04	^{66}Zn	.55E-04	^{66}Zn	.61E-05
^{67}Zn	.51E-06	^{67}Zn	.71E-06	^{67}Zn	.82E-07
^{68}Zn	.92E-05	^{68}Zn	.20E-05	^{68}Zn	.41E-06
^{70}Zn	.19E-07	^{70}Zn	.10E-07	^{70}Zn	.71E-08
^{69}Ga	.49E-06	^{69}Ga	.38E-06	^{69}Ga	.51E-07
^{71}Ga	.11E-06	^{71}Ga	.11E-06	^{71}Ga	.16E-07
^{70}Ge	.10E-05	^{70}Ge	.89E-05	^{70}Ge	.97E-06
^{72}Ge	.56E-05	^{72}Ge	.23E-05	^{72}Ge	.30E-06
^{73}Ge	.81E-07	^{73}Ge	.89E-07	^{73}Ge	.16E-07
^{74}Ge	.71E-06	^{74}Ge	.54E-07	^{74}Ge	.13E-07
^{76}Ge	.23E-07	^{76}Ge	.20E-07	^{76}Ge	.14E-07
^{75}As	.17E-06	^{75}As	.77E-07	^{75}As	.16E-07
^{74}Se	.61E-08	^{74}Se	.53E-06	^{74}Se	.53E-07
^{76}Se	.64E-06	^{76}Se	.17E-05	^{76}Se	.21E-06
^{77}Se	.63E-07	^{77}Se	.59E-07	^{77}Se	.11E-07
^{78}Se	.15E-05	^{78}Se	.34E-06	^{78}Se	.51E-07
^{80}Se	.15E-06	^{80}Se	.37E-07	^{80}Se	.17E-07
^{82}Se	.13E-06	^{82}Se	.84E-07	^{82}Se	.28E-07
^{79}Br	.10E-06	^{79}Br	.85E-07	^{79}Br	.18E-07
^{81}Br	.17E-06	^{81}Br	.48E-07	^{81}Br	.16E-07
^{78}Kr	.45E-10	^{78}Kr	.40E-07	^{78}Kr	.39E-08
^{80}Kr	.95E-08	^{80}Kr	.23E-06	^{80}Kr	.25E-07
^{82}Kr	.14E-06	^{82}Kr	.28E-06	^{82}Kr	.37E-07
^{83}Kr	.86E-07	^{83}Kr	.59E-07	^{83}Kr	.24E-07
^{84}Kr	.17E-05	^{84}Kr	.60E-06	^{84}Kr	.12E-06
^{86}Kr	.18E-04	^{86}Kr	.82E-05	^{86}Kr	.17E-05
^{85}Rb	.14E-05	^{85}Rb	.64E-06	^{85}Rb	.14E-06
^{87}Rb	.45E-05	^{87}Rb	.22E-05	^{87}Rb	.56E-06
^{84}Sr	.20E-10	^{84}Sr	.12E-07	^{84}Sr	.12E-08
^{86}Sr	.99E-07	^{86}Sr	.14E-06	^{86}Sr	.21E-07
^{87}Sr	.16E-06	^{87}Sr	.85E-07	^{87}Sr	.15E-07
^{88}Sr	.12E-03	^{88}Sr	.31E-04	^{88}Sr	.65E-05
^{89}Y	.18E-04	^{89}Y	.92E-05	^{89}Y	.20E-05
^{90}Zr	.23E-04	^{90}Zr	.28E-04	^{90}Zr	.56E-05
^{91}Zr	.46E-05	^{91}Zr	.22E-05	^{91}Zr	.51E-06
^{92}Zr	.71E-05	^{92}Zr	.31E-05	^{92}Zr	.58E-06
^{94}Zr	.98E-05	^{94}Zr	.39E-05	^{94}Zr	.56E-06
^{96}Zr	.26E-05	^{96}Zr	.86E-06	^{96}Zr	.97E-07
^{93}Nb	.38E-05	^{93}Nb	.15E-05	^{93}Nb	.23E-06
^{92}Mo	.34E-09	^{92}Mo	.26E-07	^{92}Mo	.44E-08
^{94}Mo	.55E-09	^{94}Mo	.20E-08	^{94}Mo	.46E-09
^{95}Mo	.11E-05	^{95}Mo	.43E-06	^{95}Mo	.76E-07
^{96}Mo	.54E-10	^{96}Mo	.61E-10	^{96}Mo	.33E-10
^{97}Mo	.32E-06	^{97}Mo	.13E-06	^{97}Mo	.16E-07
^{98}Mo	.78E-06	^{98}Mo	.13E-06	^{98}Mo	.97E-08
^{100}Mo	.35E-06	^{100}Mo	.11E-06	^{100}Mo	.15E-07
^{96}Ru	<E-15	^{96}Ru	.63E-12	^{96}Ru	.98E-13
^{98}Ru	<E-15	^{98}Ru	.25E-12	^{98}Ru	.45E-13
^{99}Ru	.86E-07	^{99}Ru	.36E-07	^{99}Ru	.17E-08
^{100}Ru	.54E-14	^{100}Ru	.91E-14	^{100}Ru	.54E-14
^{101}Ru	.21E-06	^{101}Ru	.70E-07	^{101}Ru	.38E-08
^{102}Ru	.59E-06	^{102}Ru	.18E-06	^{102}Ru	.12E-07
^{104}Ru	.65E-06	^{104}Ru	.13E-06	^{104}Ru	.26E-08

Table 2: Selected isotopic abundance ratios of light trans-Fe elements between Zn (Z=30) and Ru (Z=44). Comparison of Solar-System values (Lodders 2003) with the predictions of our HEW charged-particle (α-) component (see, e.g. Kratz et al. (2008); Farouqi et al. (2009) and previous results from three different nucleosynthesis scenarios, (i) the early SN neutrino-wind ejecta (Y_e=0.465) by (Hoffman et al. 1996), (ii) the γ-process in s-processed massive stars (15 $M_\odot$ model) by (Rauscher et al. 2002), and (iii) the electron-capture (EC) SNe in asymptotic giant branch stars with an O-Ne-Mg core (ST model) by (Wanajo et al. 2009).

Isotope pairs (nucleosynth. origin)	Solar System	Isotopic abundance ratios			
		This work	Neutrino-wind (1996)	γ-process (2002)	EC SN (2009)
^{64}Zn(p)/^{70}Zn(r)	78.4	79.4	/	10.5	6.6 E+7
^{64}Zn(p)/^{70}Ge(s,p)	23.3	13.6	0.39	8.63	7.7
^{70}Ge(s,p)/^{76}Ge(r)	2.84	4.61	/	2.53	2.8 E+9
^{70}Ge(s,p)/^{74}Se(p)	40.1	41.1	55.2	30.9	16.2
^{74}Se(p)/^{76}Se(s)	9.42 E-2	9.09 E-2	/	0.128	0.567
^{74}Se(p)/^{82}Se(r)	0.101	0.113	/	0.120	6.1 E+9
^{74}Se(p)/^{78}Kr(p)	2.90	11.0	41.8	10.9	7.27
^{78}Kr(p)/^{80}Kr(p,s)	0.156	0.156	/	7.40 E-2	0.245
^{78}Kr(p)/^{82}Kr(s)	3.11 E-2	2.92 E-2	/	1.97 E-2	0.654
^{78}Kr(p)/^{86}Kr(r,s)	2.11 E-2	7.9 E-4	/	5.8 E-3	5.7 E+4
^{78}Kr(p)/^{84}Sr(p)	1.52	2.77	6.94	1.83	2.28
^{84}Sr(p)/^{86}Sr(s)	5.66 E-2	4.00 E-2	/	4.05 E-2	0.240
^{84}Sr(p)/^{90}Zr(s,r)	2.25 E-2	1.3 E-4	/	2.13 E-2	2.6 E-3
^{84}Sr(p)/^{92}Mo(p)	0.340	0.344	3.1 E-2	0.467	0.442
^{90}Zr(s,r)/^{96}Zr(r,s)	18.4	5.56	/	10.4	> E+20
^{90}Zr(s,r)/^{92}Mo(p)	15.1	2.2 E+3	2.6 E+3	22.0	172
^{92}Mo(p)/^{94}Mo(p)	1.60	1.86	3.31	1.55	49.4
^{92}Mo(p)/^{96}Ru(p)	3.67	3.0 E+4	2.6 E+4 *)	3.48	2.7 E+4
^{96}Ru(p)/^{98}Ru(p)	2.97	2.57	27.0 *)	2.54	9.06

*) Average ratio deduced from the abundances given in Table 4 of Hoffman et al. (1996), where a quasi-equilibrium of ^{92,94}Mo and ^{96,98}Ru with ^{90}Zr was assumed.

Table 3: Molybdenum isotopic abundance ratios (^{x}Mo/^{97}Mo) as conventionally used in cosmochemistry for three-isotope mixing correlations to describe the nucleosynthetic origin of presolar silicon carbide (SiC) grains (see, e.g. Marhas, Hoppe & Ott (2007)). Comparison of recent data deduced from the 8 SiC X-grains measured by (Pellin et al. 2000, 2006) with the predictions of the "neutron-burst" model of (Meyer, Clayton & The 2000) and the low-entropy (S<70) charged-particle (α-)component of our HEW model.

^{x}Mo/^{97}Mo	SiC X-grains	Isotopic abundance ratios	
		This work	"n-burst" model
^{92}Mo/^{97}Mo	< E-2	4.1 E-3	1.43 E-3
^{94}Mo/^{97}Mo	< E-2	6.3 E-3	3.27 E-4
^{95}Mo/^{97}Mo	2.1	3.12	1.539
^{96}Mo/^{97}Mo	0.12	4.77 E-2	1.02 E-2
^{98}Mo/^{97}Mo	1.2	0.950	0.382
^{100}Mo/^{97}Mo	0.25	0.225	9.55 E-2